Ocean Engineering xxx (2017) 1–14

Contents lists available at ScienceDirect

Ocean Engineering

journal homepage: www.elsevier.com/locate/oceaneng

A model to map levelised cost of energy for wave energy projects

Ciaran Frost [a,*], David Findlay [b], Ewen Macpherson [c], Philip Sayer [d], Lars Johanning [e]

[a] Industrial Doctoral Centre for Offshore Renewable Energy (IDCORE), Edinburgh, UK
[b] Albatern Ltd, Midlothian Innovation Centre, Roslin, UK
[c] Institute for Energy Systems, University of Edinburgh, Edinburgh, UK
[d] Department of Naval Architecture, Ocean and Marine Engineering, University of Strathclyde, Glasgow, UK
[e] College of Engineering, Mathematics and Physical Sciences, University of Exeter, Penryn, UK

ARTICLE INFO

Keywords:
Wave energy
Economic modelling
Levelised cost of energy
Spatial analysis
Economic mapping
GIS

ABSTRACT

An economic model has been developed which allows the spatial dependence of wave energy levelised cost of energy (LCOE) to be calculated and mapped in graphical information system (GIS) software. Calculation is performed across a domain of points which define hindcast wave data; these data are obtained from wave propagation models like Simulating WAves Nearshore (SWAN). Time series of metocean data are interpolated across a device power matrix, obtaining energy production at every location. Spatial costs are calculated using Dijkstra's algorithm, to find distances between points from which costs are inferred. These include the export cable and operations, the latter also calculated by statistically estimating weather window waiting time. A case study is presented, considering the Scottish Western Isles and using real data from a device developer. Results indicate that, for the small scale device examined, the lowest LCOE hotspots occur in the Minches. This area is relatively sheltered, showing that performance is device specific and does not always correspond to the areas of highest energy resource. Sensitivity studies are performed, examining the effects of cut-in and cut-out significant wave height on LCOE, and month on installation cost. The results show that the impact of these parameters is highly location-specific.

1. Introduction

With the threat of global warming, the need to transition towards a low carbon economy is gathering pace with policy makers. Many governments and institutions have adopted targets to limit carbon dioxide emissions and utilise energy from renewable sources. Examples include the Scottish government, aiming to produce 100% of gross electricity demand with renewable forms of energy (The Scottish Government, 2015) and the EU, whose Renewable Energy Directive has targeted supplying 20% of energy demand with renewables across its member states (Parliment and Council of European Union, 2009a). Wider ranging, global action is also being taken, such as the Paris Agreement which as of December 2016 has been ratified by 120 countries.

Wave energy, while in its infancy, has the potential to contribute significant renewable capacity towards both domestic and international energy markets. Studies indicate that the global theoretical resource is approximately 2 to 4 TW (Mørk et al., 2010; Cornett, 2006; Gunn and Stock-Williams, 2012). The UK has some of the best resource in the world due to strong westerly Atlantic winds: an estimated 35% of the European wave resource (House of Commons Energy and Climate Change Committee, 2009). The practical resource that could be economically extracted from UK waters has been predicted to be between 7 and 10 GW (Boud, 2012; Mackay, 2008), with a particularly strong resource off the West Coast of Scotland (Pontes, 1998). Wave energy has a number of potential advantages over other renewables: being more predictable than wind (Reikard et al., 2015) and available at night unlike solar. However it is yet to break through into the commercial marketplace, with cost currently a major barrier. The highest energy waves are found in extremely harsh marine environments, which devices must not only survive in but also produce energy in. This throws up a number of unique engineering challenges, which require bespoke, and hence expensive technology.

Understanding the cost of any energy technology is crucial, to make sure that it is competitive in the market and allow appropriate business decisions to be made. For an expensive pre-commercial industry like wave energy it is also important as it allows the pathway for future technology development to be planned and cost reductions targeted. The future of wave energy is highly dependent on its commercial viability and

* Corresponding author.
E-mail address: ciaranjfrost@googlemail.com (C. Frost).

https://doi.org/10.1016/j.oceaneng.2017.09.063
Received 25 January 2017; Received in revised form 26 September 2017; Accepted 28 September 2017
Available online xxxx
0029-8018/

the extent to which it can compete with other sources of energy in the wider market. Economic modelling gives a way of quantifying this competitiveness, and thus designing robust models is of significant interest to the industry in the immediate term.

Economic modelling is a wide ranging topic, with a huge number of potential factors which can be considered for analysis. This means that the literature for wave energy covers a broad range of aspects. One of the earlier studies, conducted by Thorpe, was produced for the UK government to advise on the various device concepts available (Thorpe, 1999). Economic assessments were conducted by using estimates of costs and energy production, obtained from correspondence from developers. A more recent comparison study by Dalton estimated the Levelised Cost of Energy (LCOE) as a function of farm size for five device concepts off the West Coast of Ireland (Dalton and Lewis, 2011).

Because of the wider availability of data, Pelamis style devices have been commonly considered for economic assessments in the literature. While this paper is concerned with a smaller scale device, such studies should be mentioned because the underlying calculation methods are the same. The devices themselves are also similar in nature, for example both are self-referencing and rely on hydraulic power take-off (PTO) systems.

Previsic examined the commercial feasibility of a farm of Pelamis devices in California, using site specific data (Previsic, 2004). This included cost estimates from local suppliers and Monte Carlo analysis of the costs to incorporate uncertainty. A result of the study was that, while the project would struggle to compete commercially in the short term, favourable LCOE could be obtained with similar investment and learning as the wind energy industry had seen. A more recent study, conducted by Dalton et al., estimated the LCOE for the Pelamis for projects in North America, Portugal and Ireland, using a Microsoft Excel-based model (Dalton et al., 2010). Other studies include Ref. Allan et al. (2011) and Farrell et al. (2015), both of which also examine the level of present subsidy levels. The latter of these extends the analysis to revenue, using statistical analysis to estimate the confidence in a project being able to provide a significant return to an investor.

The vast majority of previous studies have been performed for single locations at a time, considering point estimates of costs and using a joint occurrence matrix to estimate energy. The limitation of such an approach is that it is difficult to know whether the point chosen is representative of the wider area, and whether it would be the optimum site for the particular device being analysed. For a developer, such an analysis gives little indication of whether the specific location accurately reflects their device's potential, and what the best location might be.

An alternative way of performing economic analyses is by repeating the calculations over multiple points, allowing the results to be mapped. Simulated metocean data is required for this, typically obtained by performing hindcast simulations with numerical wave models. While spatial methods are less accurate than single point models when considering a single location (as some costs are calculated rather than directly specified by the user), they provide a powerful indication of the best areas for deploying the device and the overall trends across the region of interest.

For wave energy, previous spatial studies have been focussed on several areas. A common theme is resource assessment studies: estimating the raw energy available in the waves to make judgements on the most suitable locations for wave energy projects (for example Refs. Pontes (1998); Iglesias et al. (2009); Sierra et al. (2013)). Some of these studies also incorporate device power matrices in the analyses, to see how the device performance matches the resource (such as Ref. Gunn and Stock-Williams (2012)). Another research theme involves using graphical information system (GIS) based methods to determine viable project locations, by taking account of spatial costs and exclusion areas. An example is Ref. Prest et al. (2007), where the effect of exclusion zones on wave energy cable routing was examined. An alternative methodology is a multi-criteria based analysis, where a selection of different locational parameters are examined and assigned a score and weighting depending on the perceived positive or negative effect on a project. These are aggregated for each point across the domain, the final scores indicating the most suitable areas for deployment. Examples for wave energy include Refs. Nobre et al. (2009); Flocard et al. (2016) and Vasileiou et al. (2017), the latter considering a combined offshore wind-wave system. While multi-criteria analyses offer a logical way to categorise sites by location, choosing the different category weightings is a somewhat arbitrary exercise and can significantly influence the final results.

The model that has been developed for this paper uses LCOE to define the most suitable wave energy project locations: by calculating spatial energy and spatial costs. It also has the ability to define exclusion zones for deployment. This approach has the advantage that LCOE is a commonly used metric that is of interest to investors and policy makers as well as developers. This is because it allows for comparison with other energy technologies and the market as a whole.

To date, there has been similar research undertaken in offshore wind (Cavazzi and Dutton, 2016) and tidal stream energy (Vazquez and Iglesias, 2016). For wave energy, there are also examples of work in this area, however there have been limitations adopted that warrant further study. Catro-Santos et al. used a GIS tool to map the LCOE around Portugal, filtering out locations corresponding to restricted areas. The wave resource was considered with spatial dependence, using mean power per metre from a resource atlas. However costs were not given spatial dependence, estimated using a high level, top down approach (considering €/kW of installed capacity), resulting in significant underestimation of LCOE for locations far from shore. An additional example, Behrens at al., focussed on the wave energy potential around Australia (Behrens et al., 2012). This study considered three different device types and determined LCOE around the coast using data from the US National Oceanic and Atmospheric Administration's (NOAA) WaveWatch III. However only sites 5 km from the coast were considered for the LCOE analysis, again with costs considered fixed (for example operations and maintenance (O&M) costs were considered per MWh of produced energy, without adjusting for local sea conditions).

The spatial distribution of costs and LCOE, as well as the methods used to calculate them, represent an area of great interest to developers, investors and policy makers. This study aims to expand on previous knowledge by presenting a model which incorporates spatial cost estimations of the export cable, installation and planned O&M into the analysis. This allows robust estimates of LCOE to be made.

The paper continues with a theory section, describing the LCOE calculation process. Section 3 then introduces the main features of the model and how the parameters are calculated in practice. A case study to demonstrate the model, focussing on the Scottish Western Isles, is described in Section 4, with the results presented and discussed in Section 5.

2. Theory

In order to calculate LCOE for a particular energy system two quantities are required: the total project cost and the total energy produced over its lifetime, both discounted to present values. As the model described by this study is spatial, the calculations are performed over a two dimensional domain, each point defined by a latitude and longitude. The metocean data that are used are hindcast data, obtained from numerical wave simulations, with wave parameter time series defined for every point.

To obtain the total energy, first a two dimensional power matrix is used to obtain a power time series for each location in the domain. Power matrices are the most common way of representing wave device output power as a function of sea state, and are derived by developers by performing numerical simulations of the device at different combinations of significant wave height, H_s and peak period T_p (or energy period, T_e). The power values can be verified experimentally, for example through tank testing or sea trials, and adjusted accordingly. Given time series of H_s and T_p, a time series of power can be obtained by using the power matrix as a lookup table, interpolating the metocean data at each time step. This interpolation is required when the metocean

Table 1
Some of the main class instances used in the model along with examples of the kind of input parameters that can be varied by the user. The overall model is typically executed using a master configuration text file.

Parameter (class)	Input variable examples
Metocean data	• Paths to data files • Spatial extents for analysis (lat/lon)
Power Matrix	• Path to data file • Maximum power limit • H_s limits
Wave Device	• Local costs • Power matrix • Export cable • Rated power • Constraints (water depth limits and restricted locations)
Export Cable	• Local costs • Cost per metre • Landing point locations
Marine Operation	• Local costs • Time periods for task (month/year) • *Hs* limit • Hours to complete task • Vessel and port options • Maximum hours for operation

values of interest are given to a higher resolution than the power matrix bins (lying between the discrete sea state values that the numerical models have been run at).

Once this process is completed for every point in the domain, the energy produced at each point as a function of time is calculated by multiplying the power at each time step by the length of the time step. This three dimensional energy is summed along the time axis to get the total energy produced in a defined time period. Typically a monthly period is chosen. For each month, the energy is then discounted to a present day value. Discounting, commonly applied to cash flows in financial analyses, is applied as energy produced in the present is considered more valuable than that in the future. The monthly energy is hence scaled with a time-dependent discount factor D:

$$D(t) = \frac{1}{(1+d)^{(y+(m/12))}}, \tag{1}$$

where d is the discount rate, m is the index of the month (one to twelve) and y the relative index of the year (starting at zero). The discount rate value reflects the amount of risk in the investment. It is often set between 6% and 10% when performing economic analyses of wave energy, the assumption being that the technology is at an early commercial level of maturity (for example Ref. Farrell et al. (2015)). The total discounted energy for each point (x, y) is determined by multiplying each monthly energy E by the discount factor for that month:

$$E(x,y) = \sum_{m=1}^{n} D(m)E(m,x,y) \tag{2}$$

This represents the denominator in the LCOE calculation. The numerator, net present cost (NPC), is a combination of the project costs that are also discounted to present values:

$$C(x,y) = C_{\text{cap}}(x,y) + C_{\text{in}}(x,y) + \sum_{m=1}^{n} D(m)C_{\text{O\&M}}(m,x,y) + D(m=n)C_{\text{decom}}(x,y) \tag{3}$$

where C_{cap} is capital cost, C_{in} is installation cost, $C_{O\&M}$ is O&M cost and C_{decom} decommissioning cost. Usually an assumption is made that capital and installation costs are incurred at the beginning of the project, before the device is operational, hence are not discounted. Decommissioning is assumed to occur in the final project month, and hence is heavily discounted. Because of this, it is assumed to be negligible for this study and set to zero.

Using Equations (2) and (3), the LCOE as a function of location, L, can be determined:

$$L(x,y) = \frac{C(x,y)}{E(x,y)} \tag{4}$$

Visualising these 2D data over the geographic domain allows the LCOE to be used as a site assessment metric, allowing the locations where LCOE is lower to be established for the particular technology.

3. The model

In order to map the LCOE for wave energy projects, a bespoke model has been created. Coded using Python, the model encapsulates the complete calculation process: from extracting the metocean data to calculating the discounted energy, costs, and LCOE. It is structured using an object-orientated approach; this is to provide coherence and modularity, as well as to take advantage of programming principles like inheritance. The OOP structure also means that it is easy to run individual parts of the code and perform analyses for specific objects, also useful for debugging. The model allows the user to define the calculation inputs using configuration text files, with results exported as GeoTIFF raster files which can be read in GIS software. Table 1 describes some of the main data classes and input parameters that the user can include for the analysis. Class instances can be stored as text files or as entries in a NoSQL database (MongoDB is currently the software of choice). Using NoSQL will allow the model to integrate with big data in future, as there are potentially a huge number of system components and subsystems that could be incorporated.

In the model, all objects which have costs associated with them inherit from a cost base class. This includes the device, export cable, ports and operational tasks. The base class has methods which allow individual cost items to be added to the object, and all of them summed by category to get total costs. The specific cost categories are defined by the user. The time period in which the cost is incurred can also be specified, as well as the frequency of occurrence, so that operational costs can be distinguished and discounted.

3.1. Pathfinding and estimating distances

Key to the spatial cost nature of the model is the calculation of distances between different points in the domain. This is achieved by applying Dijkstra's algorithm to the data (Dijkstra, 1959). The input to the algorithm is a Python dictionary structure generated from the metocean data. This stores the valid data points together, with each representing a potential site. Land points are represented by NaN (Not a Number) data and are filtered out of the analysis. The indices of the valid points are stored, each along with the indices and distances to its nearest neighbours. The distances are calculated using the haversine equation. Starting at a specific node in the graph, Dijkstra's algorithm is then applied to determine the minimum distance to each point.

Currently the algorithm is used in two instances. First to calculate the export cable routes from each point, and hence length and capital cost across the domain. Second, to calculate vessel routes from an initial port location to each potential site, to allow transit time to site and waiting time for required weather windows to be estimated.

3.2. Estimating installation and operational costs

For a particular operational or installation task, costs are estimated by first calculating the total time required to carry out the task:

$$t_{\text{task}}(x,y) = t_{\text{travel}}(x,y) + t_{\text{site}} + t_{\text{waiting}}(x,y). \tag{5}$$

here t_{travel} is the total time to travel to and from the point (x, y) in the

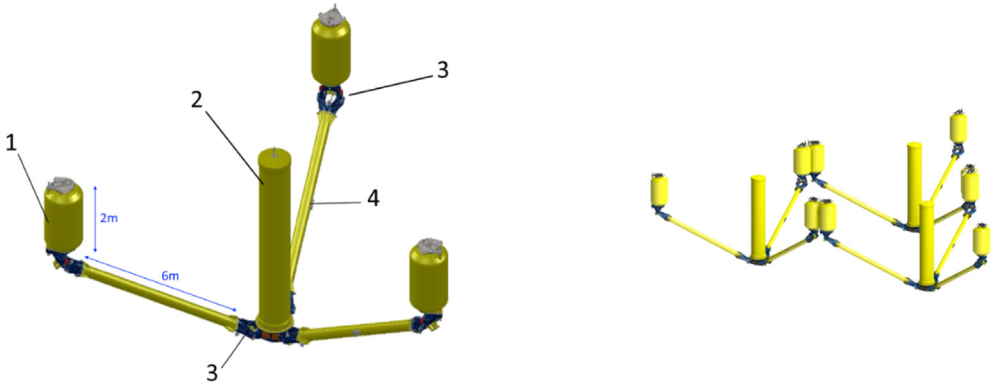

Fig. 1. The Series-6 WaveNET wave energy device. Left: A single Squid unit, made up of buoyancy floats (1), a central riser (2), hydraulic pumping modules (3) and linking arms (4). Right: An array of three Squid units, arranged in a triangular formation.

domain, t_{site} is the time spent on site carrying out the task and $t_{waiting}$ is the average time spent waiting for a suitable weather window. Calculation is performed considering units of hours.

The travel time is estimated by calculating the time to get to and from site, t_{to} and t_{from} and multiplying by the number of trips to be made, N:

$$t_{travel}(x,y) = N\left[t_{to}(x,y) + t_{from}(x,y)\right] \tag{6}$$

N depends on the number of hours that are available for a single operation, set by the user. The variables t_{to} and t_{from}, considered equal, are calculated by multiplying the distance from a specified port, d_{port} by the average vessel transit speed v_{av}:

$$t_{to}(x,y) = t_{from}(x,y) = v_{av} d_{port}(x,y). \tag{7}$$

The distance from port to each point is calculated using Dijkstra's algorithm, after adding a node into the graph at the port's location. It represents the shortest route to each location. It is assumed that all points that are at sea can be traversed, irrespective of factors like water being too shallow and land masses that are smaller than the data resolution. The former assumption is deemed sufficient for the case study presented in Section 5, due to the fact that the device and vessels required are small. Improvements to the pathfinding algorithm, to take account of these factors, is considered to be future work. Multiple ports can be specified for a particular task. In this case the port which is closest to each location is used, essentially an optimisation for shortest port distance.

The time on site required to carry out the operation, t_{site}, is defined by the user. This is independent of location in the current model, although could be made spatially dependent in future to account for the fact that operations may take longer in more extreme conditions.

Lastly, to calculate $t_{waiting}$ from Equation (5), the length of the weather window is required. The assumption is that this is equal to the time t_{site}. By defining a H_s limit for the task, the maximum H_s which the task can be performed in, the waiting time is calculated at each point in the domain using t_{window} along with the statistical methodology presented by Ref. Walker et al. (2013). This is based on the National Maritime Institute (NMI) method, a modified version of Graham's method that was originally proposed by Ref. Kuwashima and Hogben (1986). It is a recommended protocol from the EquiMar Project (Stallard et al., 2010). While it is not as rigorous as time series based methods, it is well suited for the model as the calculation can be performed relatively quickly over a large number of points, without needing to iterate through potentially thousands of time series in turn.

Waiting time is calculated for the particular month in the project lifecycle that the operation takes place in, by isolating that part of the time series and performing the statistical analysis. Tasks can be designated as pre-project; in this instance a representative month is chosen for the analysis but the final cost is not discounted. This is the typical approach taken for installation tasks. Currently H_s is the only environmental constraint that is considered for calculating $t_{waiting}$. In reality, other factors like T_p and wind speed will also dictate weather window availability and are planned for future case studies.

After calculating $t_{waiting}$, the total task duration using equation (5) is obtained. If at a particular point the total task duration exceeds the total time available in the month, the operations is deemed not possible and is given a value of NaN. Finally, the total cost of chartering the operation vessel can be calculated, C_{vessel}. Assuming that the vessel is contracted on a daily basis, t_{task} is rounded up to the nearest day and multiplied by the vessel charter rate c_v:

$$C_{vessel}(x,y) = c_v t_{task}(x,y). \tag{8}$$

This vessel charter cost can be combined with additional, task specific costs to give an overall cost for the task. Examples of these costs could be the costs for equipment to carry out the task, replacement parts or port fees.

3.2.1. Export cable installation

Because the export cable installation is carried out at multiple points across the domain, along the cable route from shore to site, the calculation procedure is different to standard, single point, tasks.

For a given site point, all of the intermediate points along the cable route are stored. First, the time for the vessel to get to the cable landing point is determined, as previously described. Next, the total time to install the cable is calculated, using the cable length L_c:

$$t_{install} = v_{install} L_c, \tag{9}$$

where $v_{install}$ is the cable installation speed, defined by the user.

The length of the weather window required to install the cable is set equal to $t_{install}$, the assumption being that the cable must be fully installed in a single operation. The corresponding waiting time to carry out the whole operation is determined by first using the aforementioned NMI method to calculate the waiting times for every point along the cable route, using $t_{install}$ as the window length. The waiting time selected is the maximum waiting time calculated across the route, corresponding to the point with the most extreme conditions. This assumption is somewhat pessimistic in nature, as it essentially regards all of the points along the route as having the same weather conditions as the most extreme point.

Lastly the time to get from the final point, at the site itself, back to the port is calculated from the distances. Thus, the time needed to charter the vessel can be calculated as in Equation (5), and the charter cost obtained.

3.3. Deployment constraints

As well as providing quantitative calculation results for each domain point, the model can also tell the user the points where deployment is not possible. These constraints on deployment are important to include so

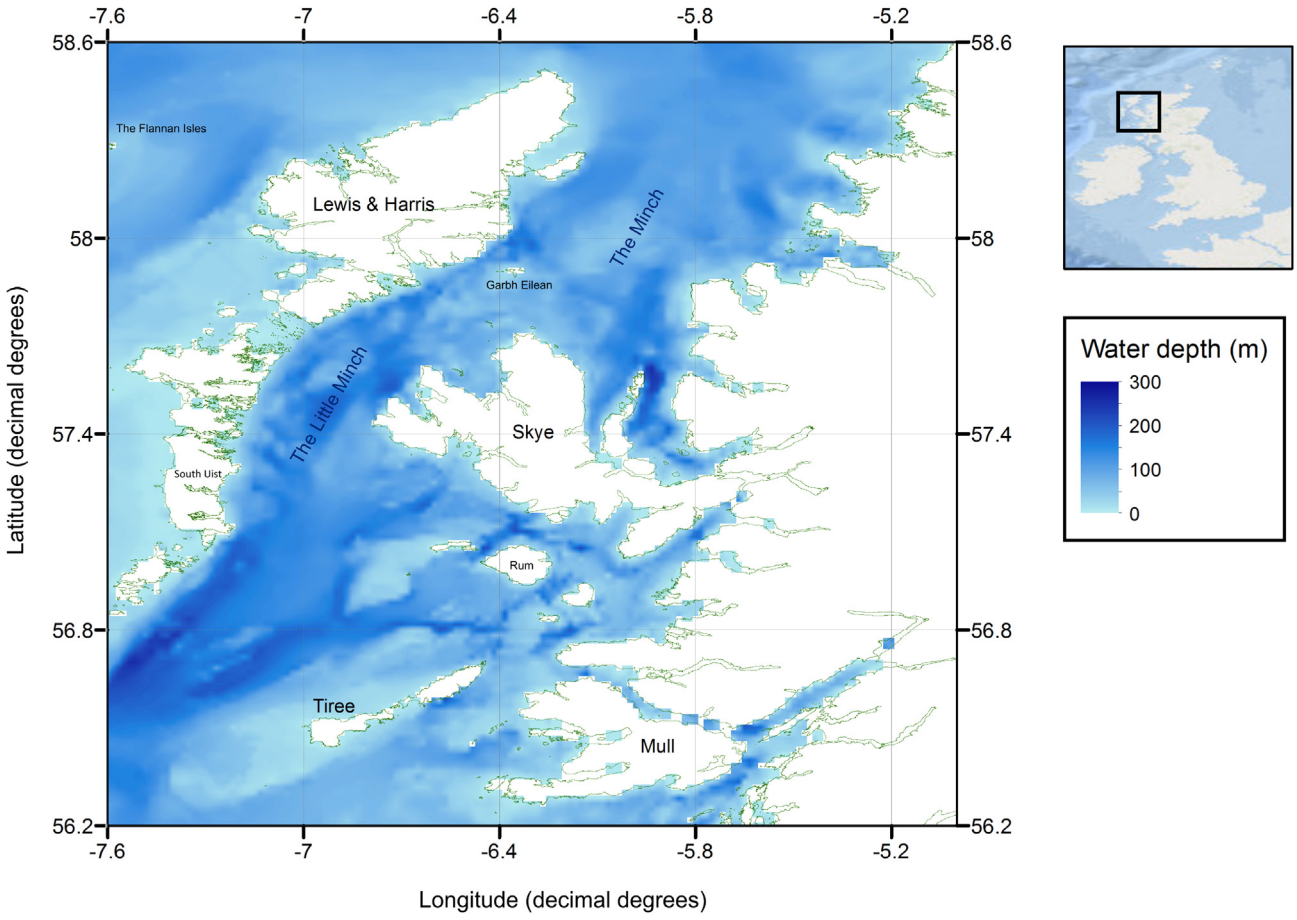

Fig. 2. The domain which was considered for this study. The location, encompassing the West Coast of Scotland, includes the Inner and Outer Hebrides.

that users can get a realistic impression of the real world locations that could be available for a given project.

The inequality defining the constraint and the data that the constraint is applied to are defined by classes within the model. Current constraints supported by the model include maximum and minimum water depth, export cable length, distance to the nearest port and protected environmental areas. The former constraints are based on simple inequalities, screening out the locations if numeric values lie outside of user-specified ranges. The latter constraint is achieved by checking if the points lie within geographic boundaries defined within third party vector files, achieved by loading the vector data into Python. After determining the constraint locations, the model then outputs raster layers for each constraint as well as a combined layer which assigns unique pixel values to points where multiple constraints are present.

4. Case study

4.1. Model inputs

To demonstrate the model, sample results are presented. These were generated considering a specific wave energy device, the Series-6 WaveNET, which is designed and manufactured by the industrial project sponsor Albatern Ltd. The small scale device, shown in Fig. 1 is modular and array based. It floats on the water surface and generates electricity with a hydraulic PTO system, driven by the relative motion between the central riser and buoyancy floats. The array units, known as Squids, are each rated at 7.5 kW. The array size chosen for the analysis was a triangular, six unit array rated at 45.0 kW.

The power matrix representing the device was provided by Albatern, having been generated in-house by performing time domain simulations using Ansys AQWA. The device components were modelled as rigid bodies, subjected to hydrodynamic loadings calculated by Morison's equation. Analyses were performed over a range of irregular sea states, with power production determined by examining the external forces opposing the device motion. The power matrix values are idealised, representing raw mechanical power (hydraulic, mechanical and electrical losses are not considered) and it is yet to be experimentally verified. Reductions in energy production due to device failures and PTO efficiency were not included. This was because the spatial nature of these variables is complex and considered outside the scope of this study. In this baseline scenario, the assumption was made that the device could operate in any sea state, limited only by its rated power.

The location that was chosen was the Scottish Western Isles, shown in Fig. 2. This area, encompassing the Inner and Outer Hebrides, is known for its wave energy potential. Metocean data were provided by Albatern, originally purchased from Metocean Solutions Ltd. Metocean Solutions generated and internally validated the data using SWAN (Simulating WAves Nearshore) (Booij et al., 1999). The domain spans the area −5.0 to −7.6°W longitude and 56.2 to 58.6°N latitude, at a resolution of 1/60° in both directions. The dataset time resolution is 3 h. A device lifetime of ten years was assumed, using ten years of hindcast metocean data for the analyses (from 2000 to 2009). Assuming a relatively mature level of technology, a discount rate of 8% was applied. Both of these parameters are in line with estimates made in the literature (for example Refs. Allan et al. (2011); Previsic (2004)).

Three constraints on device location were considered. Two of these were related to the bathymetry, namely that the device must be deployed in water deeper than 20 m but shallower than 150 m. The lower limit is related to the draft of the device, to prevent it from colliding with the seabed during operation. The upper limit, more arbitrary in nature, was

Table 2
The main properties of the installation tasks considered for the case study.

Installation task	Device	Mooring	Export Cable
Time of year	March	March	March
H_s Limit (m)	2.0	1.5	1.5
Vessel class	Multicat	Multicat	Cable laying
Vessel charter (£/day)	1,500	1,500	4,000
Time on site (h)	4.0	2.0	N/A
Mobilisation cost (£)	3,000	3,000	6,200
Demobilisation cost (£)	3,000	3,000	6,800

Table 3
The main properties of the planned operations considered for the case study.

Task name	Servicing (collection)	Servicing (redeployment)	Mooring inspection
Period (years)	2	2	1
Time of year	June/July	June/July	June
H_s Limit (m)	1.5	1.5	1.0
Vessel class	Multicat	Multicat	Multicat
Time on site (h)	2.0	2.0	3.0
Cost (£/operation)	1,300	300	1,500

set to take account of the difficulties and extra costs that would be expected with installation and mooring system design at large depths. The third constraint was that the device could not be deployed in a special protected area (SPA) (Parliament and Council of European Union, 2009b) containing a marine component; this follows the approach taken in (Vasileiou et al., 2017). The SPA locations were downloaded from the Joint Nature Conservation Committee website (Joint Nature Conservation Committee, 2009). While being located within an SPA would not automatically prevent a marine license from being obtained, it is assumed that the additional steps required to get the project approved would put off the developer and get them to scope out other areas first.

The project capital costs that were considered were the cost of the device, mooring system and export cable to shore. The specific cost values are not presented in this paper as the numbers are commercially sensitive. The mooring system is made up of three catenary lines, each secured to the seabed with a drag embedment anchor. Land based costs, for example associated with the electrical connection to the grid, have not been included. This is because calculating the spatial dependence of these costs is currently outside the scope of the model. The case study assumes that the cable for each point is landed at the nearest land point, to provide a general overview. In addition, the same export cable model is used at all points in the domain. In reality, locations further offshore would require a more expensive cable to reduce losses. Efficiency losses in transmission are not considered in the case study.

For the installation cost, three distinct tasks were considered: installing the device, the mooring system and the export cable. While the frequency-based methodology does not consider the exact timing of the tasks within the month of install, in reality the mooring system is installed first, in a single operation, followed by the cable and devices. The device installation process includes towing a single module out to site at a time and connecting it to both the mooring system and the neighbouring modules. Table 2 shows the main properties of the tasks. These numbers are estimations, and are included purely to demonstrate the model capability. They are based on a degree of learning in operations. For instance, in the case of the device and mooring install, larger vessels than Albatern currently use are considered, which would offer greater stability in more extreme sea states. Stornaway and Mallaig were selected as the potential operations ports, as both are encompassed by the domain and deemed to have the necessary facilities for such a project. No additional costs related to port use were included.

The device and mooring vessel mobilisation and demobilisation costs were each based on two days of charter. The export cable vessel costs

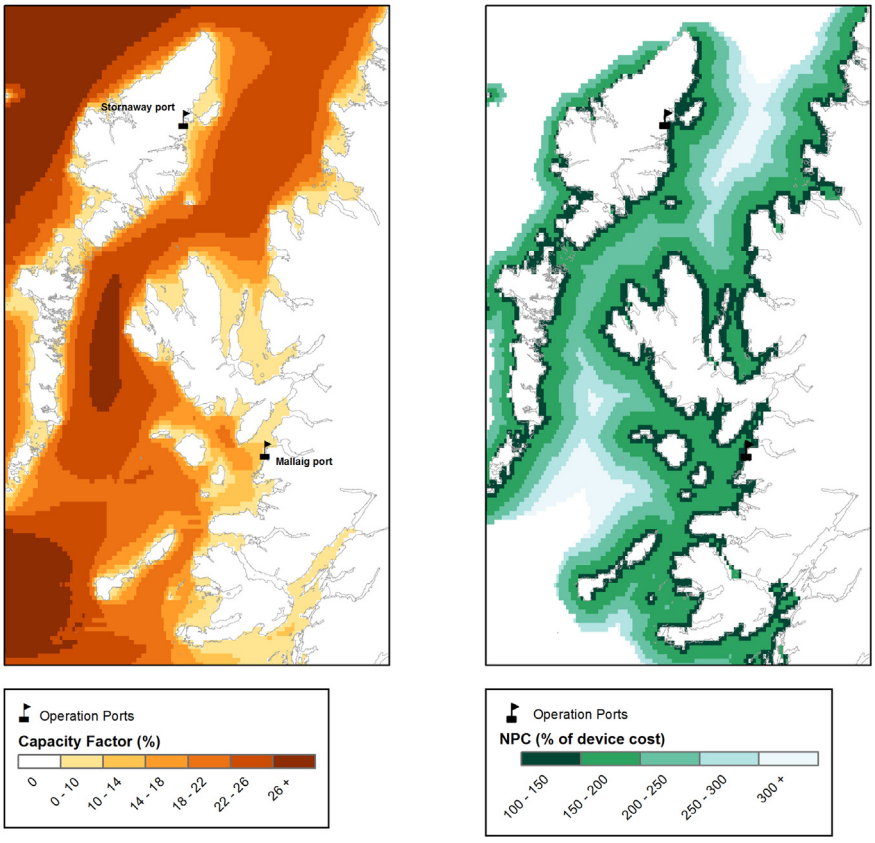

Fig. 3. Left: The device capacity factor over the extent of the domain. Right: The total project net present cost (NPC) over the domain. The cost data, non-dimensionalised to preserve commercial confidentiality, are represented as percentages of the total device capital cost.

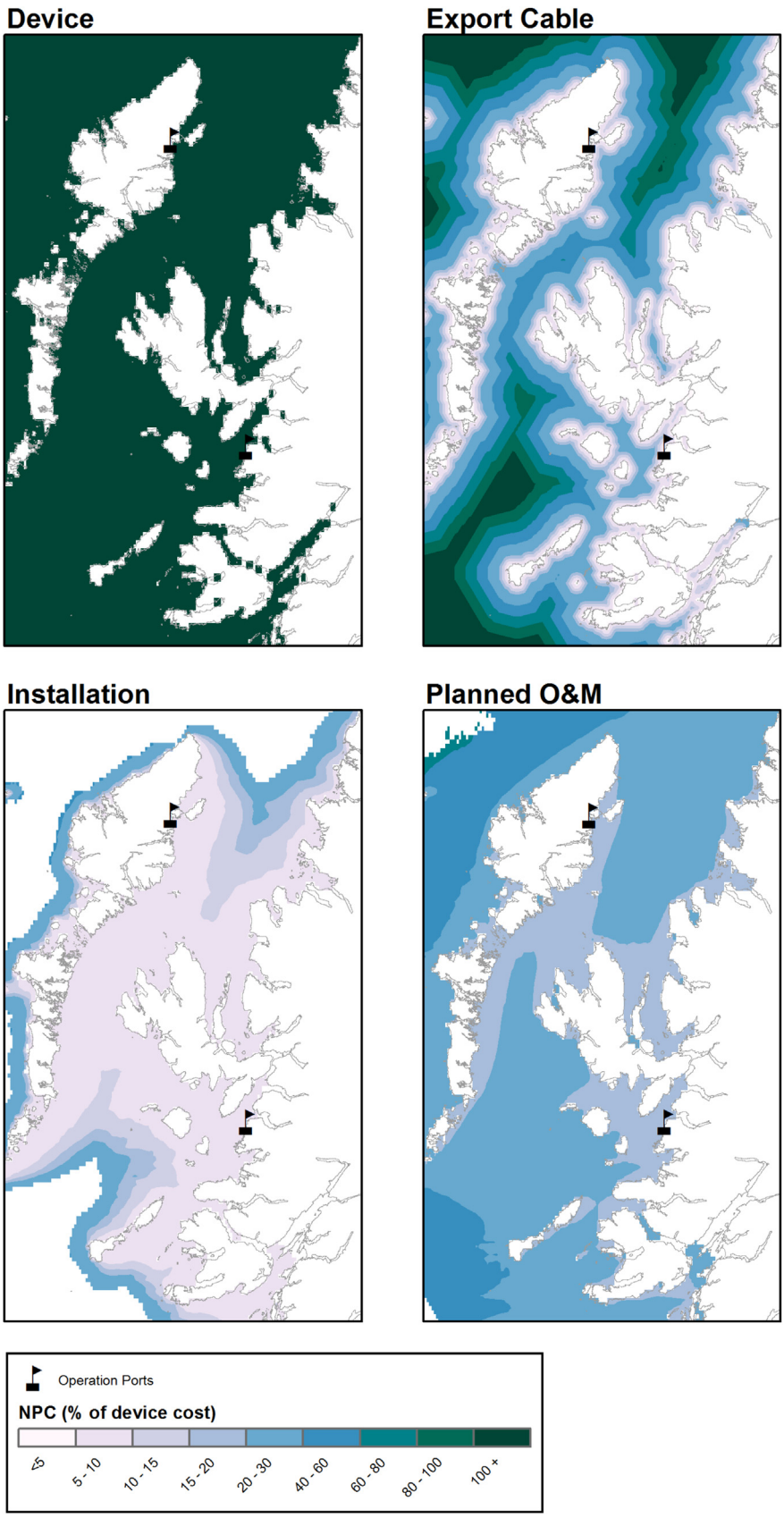

Fig. 4. The net present costs (NPC) of the four main project components that were considered for the case study. The export cable cost includes the capital cost only (the installation cost is included in the installation figure) and the cable is modelled as running to the nearest land point. The data are represented as factors of the device capital NPC, to preserve commercial confidentiality.

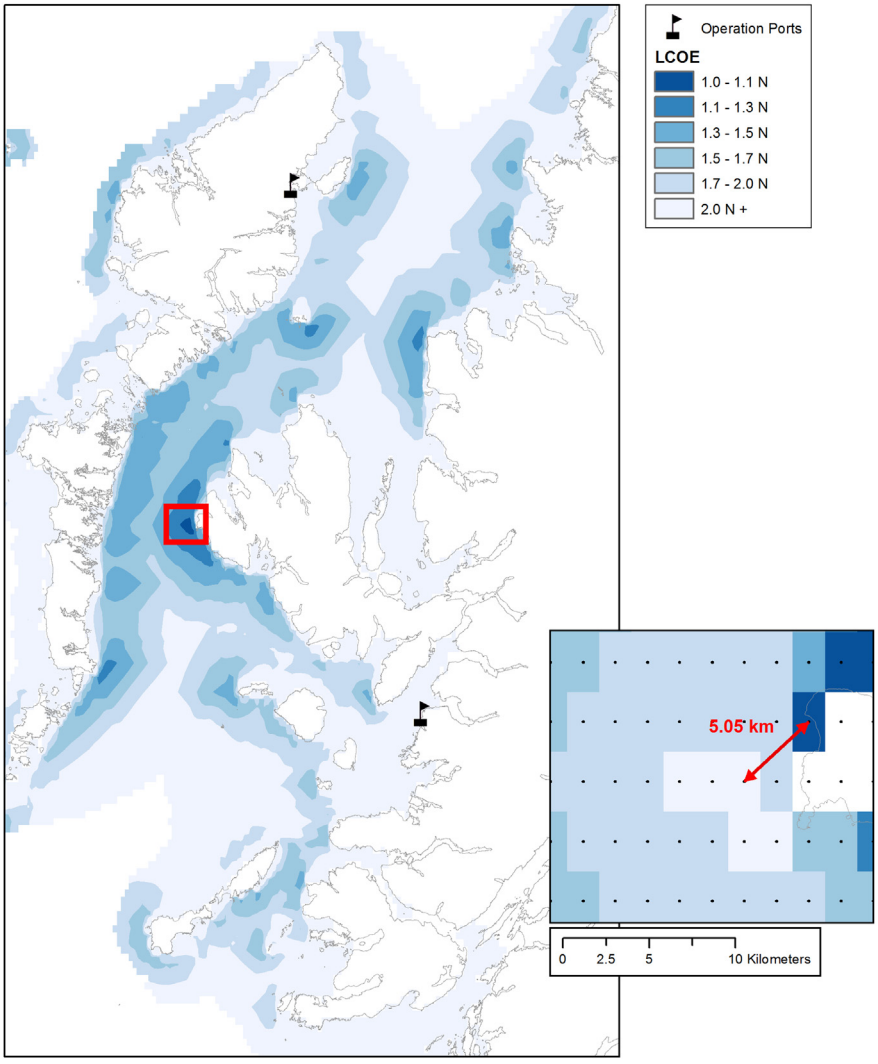

Fig. 5. The LCOE over the domain for the baseline scenario. The lowest LCOE for the Series-6 device was found to be in the Little Minch, off the West Coast of Skye. The inset shows a close up of this area at the original data resolution (without interpolation) to illustrate the high spatial variability of the data. The data, represented as factors of an arbitrary constant *N*, have been non-dimensionalised to preserve commercial confidentiality.

were based on a quotation from Albatern for a recent project, which the charter rate was also inferred from. As the rated power of the device is relatively low, a light 1 kV untrenched cable can be used which accounts for the relatively low cost. In reality, larger trenched cables would be required further offshore to provide protection and minimise losses but this is not considered for the case study. In total eight installation operations were considered; these included installing the mooring system, the export cable and each of the six Squid modules, all in the month of March (using representative data from the year 2000). Because the weather window and waiting time estimation is frequency based, specific scheduling of the tasks was not considered, nor the potential issues of overlap in vessel hire (each task is considered independently).

Planned O&M costs were also considered for the case study, their input properties shown in Table 3. The original numbers can be found in Ref. Gray (2017) with slight modification for the case study. As there is limited operational experience associated with the device, they are estimates of the operational procedures at a commercial maturity. Two tasks were considered: a routine service of each Squid module every two years, and an annual inspection of the mooring system. The former task is modelled as two components: collecting the Squid unit and reinstalling it, with three Squids serviced in June and three in July. No power losses associated with the servicing downtime were considered, as this is currently not supported in the model, but will be included in future work. Downtime would widen the spatial variation seen in the model, as exposed locations would be hit by reductions in energy output as well as higher costs. The case study also does not include unplanned maintenance costs, typically modelled with Failure Modes and Effects Analysis (FMEA), as these are currently outside of the model functionality.

4.2. Analysis procedure

First the model was executed using the baseline data described in the previous section. Each year of metocean data is stored in a separate file, they are loaded and stacked together within the model at runtime. First the model performs the energy analysis, obtaining the lifetime energy produced at each location. Next, the cost analysis is performed by iterating down through the different nested class instances making up the model, performing the necessary calculations and aggregating the category totals. Each total is then divided by the total discounted energy to get the contribution of each category to LCOE. Once these analyses are completed, the constraint layers are derived by the model and all of the results are exported to GIS raster files.

To demonstrate the capability of the model, three different sensitivities to the case study were examined. First a cut-in H_s was applied to the device, to see how much this would increase the LCOE across the domain. Two cut-in values were applied to the baseline model: 0.5 m and then

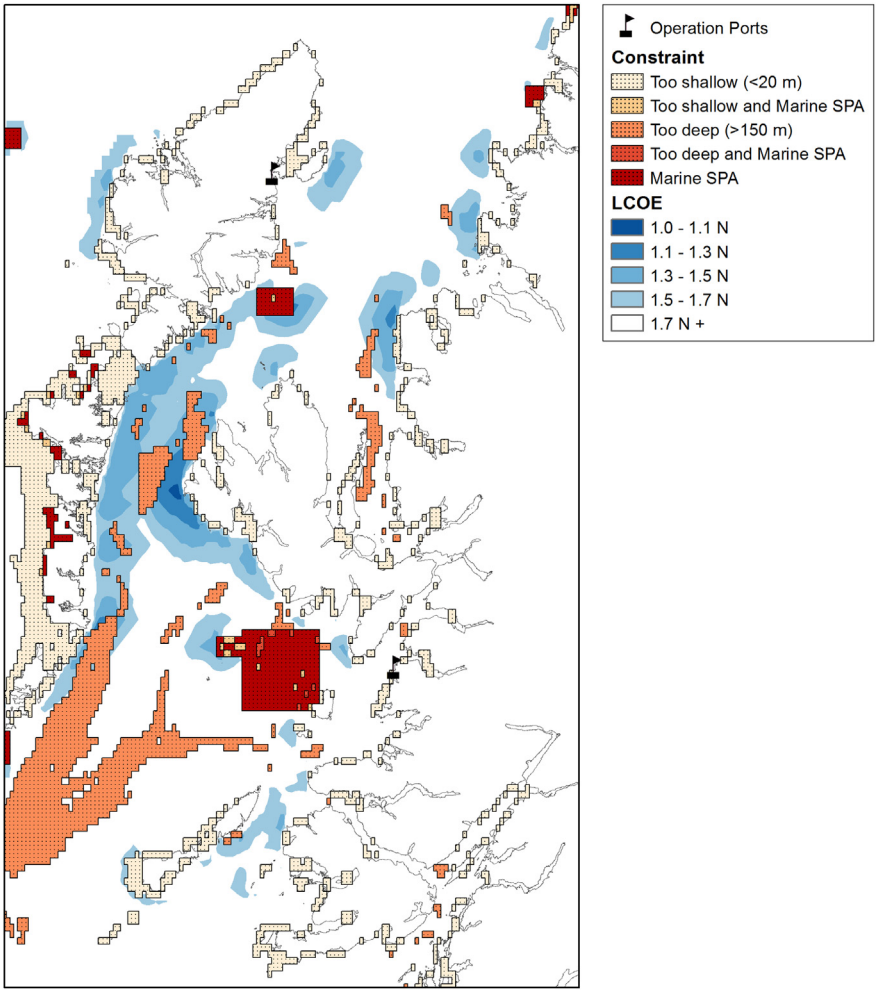

Fig. 6. The deployment constraints laid over the baseline LCOE from Fig. 5. From three original constraint categories, five constraint combinations were identified.

1.0 m. This mimics the behaviour seen in the real system, where at low wave heights the hydraulic system cannot build up enough pressure to generate power. Next, two values of cut-out H_s were applied: 7.0 m and then 6.0 m, again to see the level of increase in LCOE across the domain. This models the device going into a non power producing survival mode in extreme conditions. Lastly, the sensitivity of installation cost to the month of install is presented. Four months were considered: February, April, July and October, to show the variation throughout the year (data from the year 2000 were used to represent the months).

The majority of the results presented in the proceeding section were interpolated within ArcGIS, to make the data trends more clear. The maps in Fig. 3 are presented without interpolation, to display the underlying data resolution. In addition, most of the maps are presented with the data non-dimensionalised as the results are commercially sensitive to Albatern. Maps concerning costs have been normalised to the device capital NPC, as this provides an appreciation of the relative cost proportions. For the overall LCOE map, the values were divided through by an arbitrary factor. The colour scales used to present the data were chosen from those suggested by the ColorBrewer 2.0 website (Colorbrewer 2.0, 2013).

5. Results and discussion

Fig. 3 shows the capacity factor of the device and the NPC for the total project that were calculated for the baseline case study. The NPC, represented in terms of the device cost, has an underlying trend that would be expected: the value increasing both further from shore and in more exposed locations, for example on the west coast. The plot of capacity factors shows that, in general, the device produces more energy further from shore, and to the west of the domain where the locations are more exposed to the prevailing Atlantic westerly waves. However, somewhat counter-intuitively, there are also high capacity factors seen in the Minch and Little Minch (the Minches) which are relatively sheltered areas of water.

The reason for this is due to the sensitivity of the device performance to wave period, and not just significant wave height. While higher period waves are more energetic at a given wave height, the device is less able to convert this into useful energy. This is because the device is relatively small and in these large swell waves the power-producing components tend to heave as a unit with the waves. In higher frequency waves, typically wind sea waves, the different components instead move relative to each other which is what primarily drives the hydraulic pumping modules and power production.

The fact that the Minches are such a good source of energy for this device concept is also interesting from a cost perspective, as the plot of NPC indicates. The less extreme conditions mean that, in reality, the device would be easier to deploy, install and access for maintenance, with more weather windows available. While not quantified in this case study, the lower frequency of storm events and extreme conditions would reduce the extreme loads seen by the device components and mooring system, improving reliability compared to more exposed locations. The energy result, that some more sheltered sites outperform higher energy sites in terms of energy production, highlights a main advantage of using such a spatial approach. Such conclusions would be difficult to formulate by performing the analysis for select individual points, without being

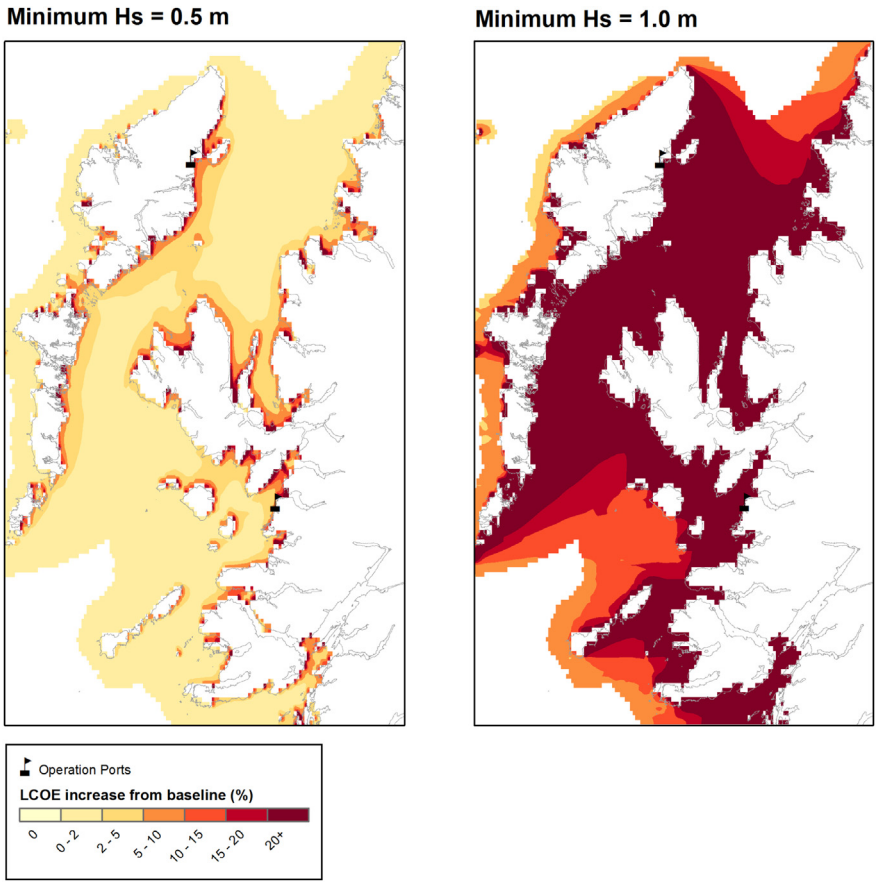

Fig. 7. The percentage increase in levelised cost of energy (LCOE) caused by introducing a cut-in significant wave height to the device in the model. Left: cut-in value of 0.5 m. Right: cut-in value of 1.0 m.

able to visualise the wider trends.

A more detailed breakdown of the costs is presented in Fig. 4, where the four main cost categories that make up Fig. 3 are displayed separately. The device capital cost is spatially static and is the largest cost over the majority of the domain. This is followed by the export cable cost, which varies from less than 5% of the device cost close to the shore to exceeding it at very large distances. At these latter locations, a larger system capable of producing more energy would be better suited, where this increased cost could be partially offset.

The value of installation cost is largely insignificant over the domain, particularly in the Minches where the cost is less than 5% of the device cost. At these locations there are numerous weather windows, meaning that vessel waiting time is low and hence the total days of charter required are low. The main impact that installation has is on the size of the domain itself, mainly driven by the export cable installation. For the more westerly locations, the time required for the installation exceeded the time available in the month, making device deployment impossible.

Similar trends to the installation costs are seen in the planned O&M costs, as these also rely on calculation of weather window waiting time. However, because summer months were chosen (as opposed to March) much more of the domain is available. Because operations occur throughout the ten year lifetime the values are significantly higher than the installation costs, typically between 20 and 60% of the device cost.

A map of the total LCOE for the case study project is shown in Fig. 5. This is essentially the ratio of the two plots from Fig. 3, but with the capacity factor plot represented in terms of total energy output. By visualising the data in this way, several hotspots of low LCOE can be seen. These include a number of locations along the West Coast of Lewis and Harris, to the south east of South Uist and the West Coast of Skye in the Little Minch. Also of note is the sometimes dramatic spatial variability in results, illustrated by the inset figure. Deploying the device just 5.05 km south west of the more sheltered location reduces the LCOE by 72.5%. This highlights the benefits of adopting a spatial approach for site assessment and scoping, and would be further improved with higher resolution data.

It can be seen that some of the lower LCOE areas are those which would not usually be thought of as being good for wave energy, as also implied by the capacity factor plot from Fig. 3. The main example is the Little Minch, where the lowest LCOE in the whole domain is found. The best locations will be strongly device specific, not only due to differences in the power capture characteristics but also due to the differences in costs incurred by the developer. These costs will depend on factors like water depth, mooring type, the type of vessels required, where the port of operations is and the consenting process that might be required.

As a significant spatial cost factor is the export cable, in this case modelled as the shortest distance to shore, there are some hotspots which in reality would not be so suitable for wave energy due to lack of electricity demand (for example the Flannan Isles which are uninhabited). Additionally, the location of the electrical infrastructure on land has not been considered, so in reality some locations would not be feasible as they would be too far from the grid, making projects very costly. The nature of the seabed, in particular the slope, will also have a large impact on the route that the cable can take. This could be incorporated into future case studies if higher resolution bathymetry data were available, as at the current resolution the points are too far apart to see significant gradients.

Fig. 6 shows the LCOE map from Fig. 5 but with the constrained deployment locations imposed over the top. Including combinations of

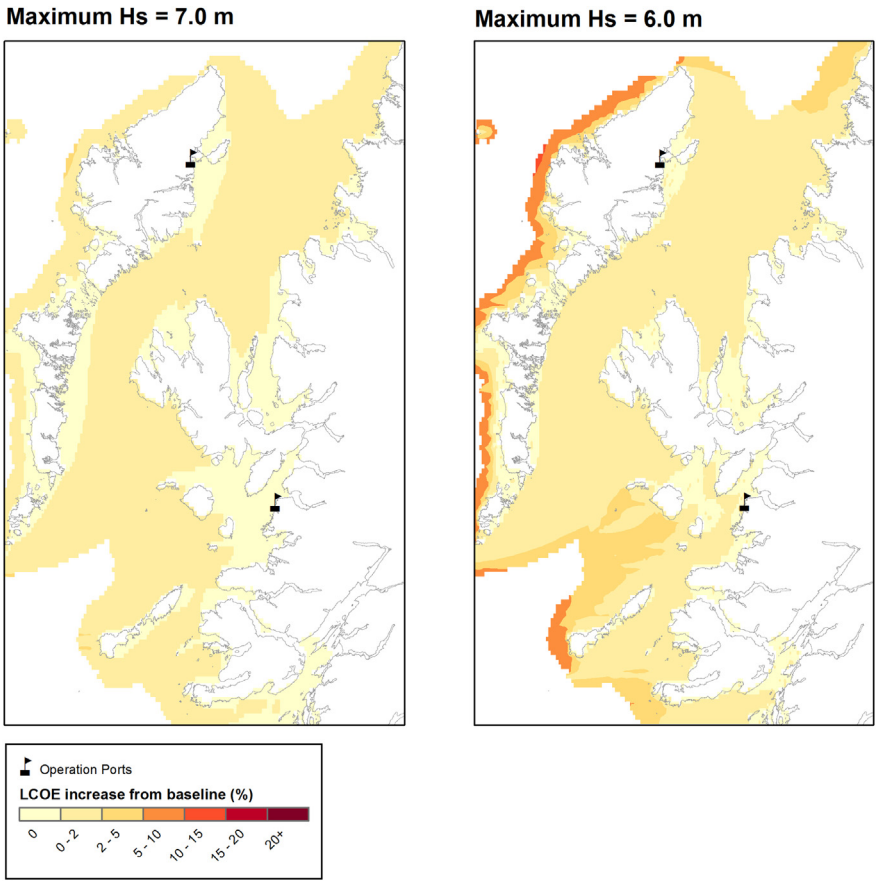

Fig. 8. The percentage increase in levelised cost of energy (LCOE) caused by introducing a cut-out significant wave height to the device in the model, representing the device going into a non-power producing survival mode. Left: cut-out value of 7.0 m. Right: cut-out value of 6.0 m.

SPA and water depth constraints, there are five constraint categories in total. The map shows that the lowest LCOE areas are largely clear of the constraints that were defined. There is a deep trench to the east of the Little Minch hotspot, however as the export cable runs to the shore on the West Coast of Skye this would not be an issue. Unfortunately much of the South Uist hotspot is located in deep water, however there are still a couple of decent points neighbouring the deep section. Most of the shallow regions coincide with very sheltered regions where projects are less economically feasible. The main exception to this is the large shallow zone off the West Coat of Tiree which is effectively blocking off any site of interest. The SPA constraint also has a fairly low impact on project locations. While there are unavailable hotspots around the Flannan Isles and Garbh Eilean, both of these are uninhabited and so do not represent practical markets. Conversely, the Isle of Rum is inhabited but does not present any sizeable hotspots (see Fig. 5) so again is not of great loss.

5.1. Sensitivities

5.1.1. Cut-in Hs

Fig. 7 shows the percentage increase in LCOE when introducing a device cut-in H_s. The impact of the 0.5 m cut-in is largely minimal because the areas that see the biggest increases in LCOE already had high LCOE so were not of commercial interest. The majority of the sites, including the hotspots previously mentioned, see increases in LCOE of less than 4%. However, increasing the cut-in to 1.0 m has a very significant impact on the LCOE in these regions. The sites in the Minch rely on sub 1 m H_s sea states for a large proportion of their energy production, so being unable to produce power for these occurrences sends the LCOE soaring, by over 20% across much of the area. Even for sites in more exposed locations where the majority of energy is from sea states above 1 m H_s, such as the West Coast of Harris, the projects typically sees increases of 6% and greater.

While the cut-in H_s is something which is not easy to design for, dependent on the PTO system architecture, it can have a significant impact on the system LCOE. This is particularly the case for a small scale wave energy device like the Series-6 WaveNET that is designed for calmer wave climates.

5.1.2. Cut-out Hs

Fig. 8 shows the increase in the baseline LCOE from introducing a cut-out H_s to the device. At a 7 m H_s cut-out, the increase in LCOE is minimal. While there is a slight increase of 1–3% for the more exposed western locations, across most of the domain there is little to no change. This implies that the contribution to energy production from waves above 7 m is very low. Reducing the cut-out threshold to 6 m sees a much greater increase in LCOE for the exposed locations, over 9% in some cases. This contrasts sharply with the Minch area, most of which sees less than 1% increase in LCOE. Examining this sensitivity emphasises the advantage of sheltered sites for this device concept. The hotspots to the west of Harris take a large hit to availability from being unable to operate in these sea states, typically above 7%, compared to hotspots of an equivalent scale in the Minches (for example to the east of Stornaway there is a 0–1% LCOE increase).

Ultimately, the level set for the cut-out H_s will depend on the device design and should largely be a cost based decision. While a better engineered device might be able to produce power in harsher conditions, if the capital cost is too high then it will be difficult to economically compete. Conversely, a cheaper device might not be able to survive to the same degree but may be able to produce energy at a lower LCOE by virtue of cheaper costs.

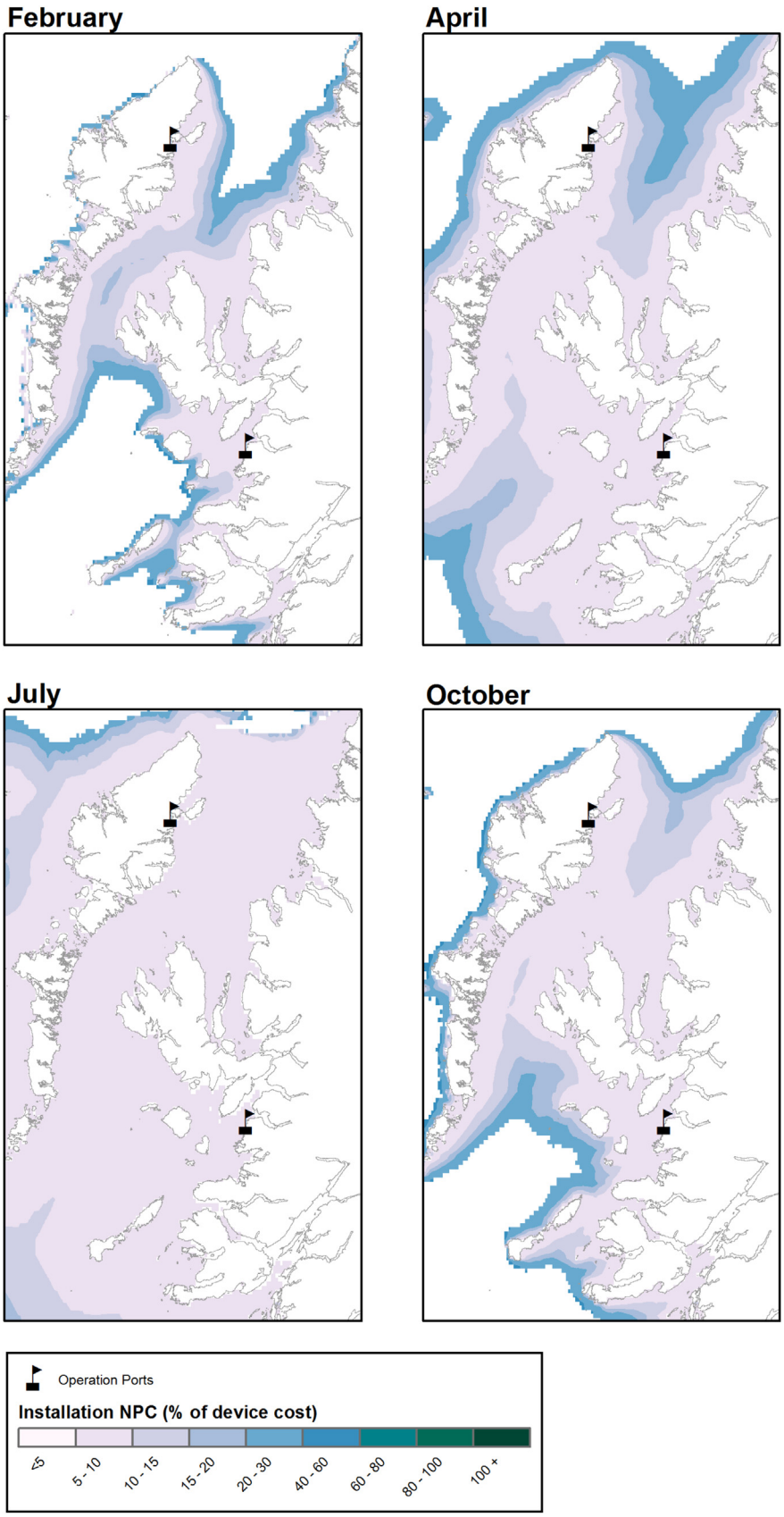

Fig. 9. The installation net present cost (NPC), considering installation occurring in different months. The data are given in terms of percentages of the device capital NPC.

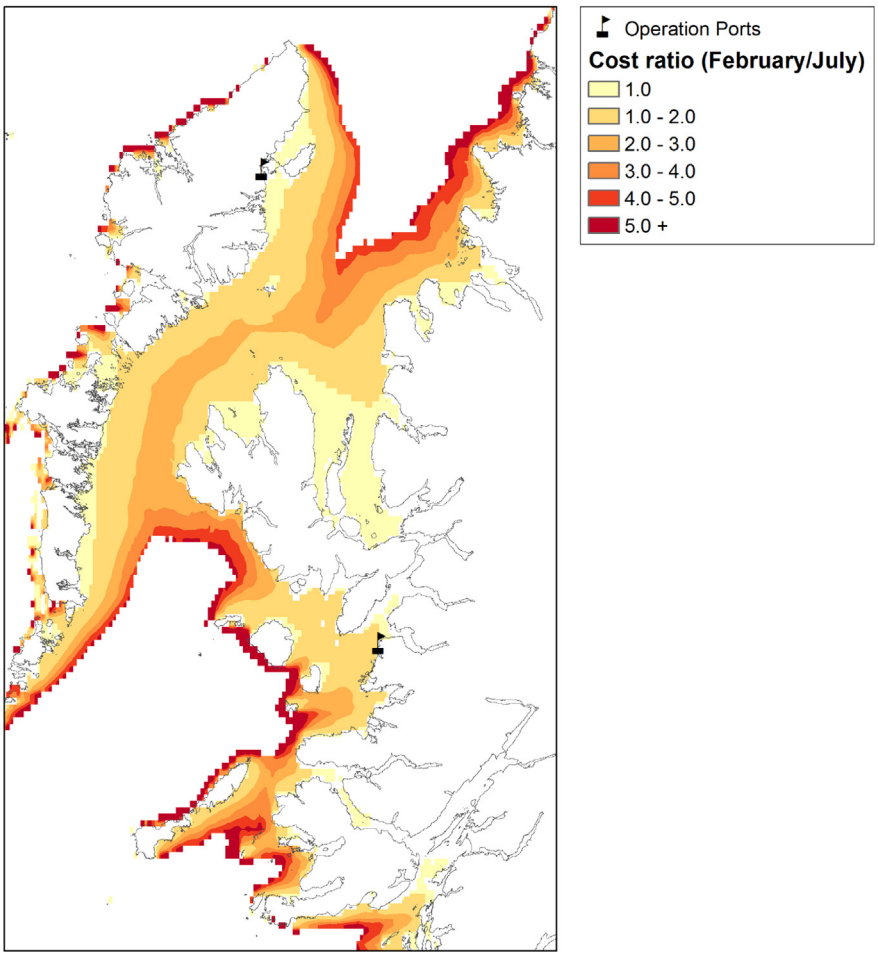

Fig. 10. The ratio of project installation cost for a February installation over a July installation.

5.1.3. Installation period

Fig. 9 shows the variation of installation cost with the month of installation. For all four of the months presented, the installation cost is higher for the more exposed locations to the west. This is because the waiting time for suitable weather windows is higher, meaning that the installation vessels need chartered for longer. The distance to these points is also a factor. As they are quite far from the ports, multiple trips were needed for operations, again increasing the time required for vessel charter.

In July, it is possible to install the device almost everywhere within the domain. Relatively low costs are seen off the West Coast of Lewis and Harris, indicating that the waiting times for weather windows are short, comparable to those seen in the Minches. This contrasts with the other months presented, particularly February, where over much of the domain a project would not be viable due to the extreme sea conditions. The cost variations are more clear in Fig. 10, where the cost ratio between installing in February and installing in July is presented. In the Little Minch and more sheltered areas the cost difference is typically less than three times, however this rises to over five times to the west of Lewis and to points in the south west of the domain. This shows that the time of year for installation is a much greater factor for some areas then others, and highlights that the spatial mapping approach is a good way to identify the most important economic drivers for different locations of interest. For example, the sensitivity indicates that a summer install would be an effective strategy to keep installation cost low for a project to the west of Lewis, however would be less important for a project to the east of South Uist where other factors might take priority.

6. Conclusions

An economic model has been presented that can perform spatial calculations of energy, cost and LCOE for wave energy projects. Energy is obtained from interpolating hindcast wave data against a device power matrix and spatial estimates of export cable, installation and planned O&M costs are made by applying Dijkstra's algorithm and statistical wave analysis. While the methodology does rely on a number of assumptions, for example assuming the shortest distances between points for path finding, the results show that it is a powerful way of gaining insight into economic performance.

Such a model could form the basis of a wider site assessment tool, not just of interest for developers but also to investors and policy makers to help inform business decisions and identify target markets. The paper adds to current knowledge by providing a high resolution, robust way of estimating locational export cable, installation and O&M costs, driven by real world data and project considerations.

The case study, using data from a developer, has highlighted that the best siting of a particular device does not necessarily correlate with the highest energy wave resource. The lowest LCOE hotspot that was found, in the Little Minch, is relatively sheltered and would not be traditionally thought of as a decent site for wave energy. Ultimately the best location will depend on the device and specific technology, and the ability to provide such an overview is why spatial analysis is such a useful tool. The sensitivity analyses showed that the impact of cut-in, cut-out and installation month are very much dependent on location. They also showed that the methodology provides a good way of identifying the biggest cost drivers for the particular region of interest, meaning that a

project can be specifically tailored to optimise economic performance.

6.1. Future work

There are many ways in which the model could be improved and the case study expanded on. To allow unplanned O&M costs to be incorporated, a reliability module could be incorporated as an add-on to the model. Using component failure rate estimates, O&M strategy and cost could be determined over the domain using FMEA analysis. Additionally, the model could be expanded to include calculation of revenue and analysis of the different investment options that could be made for a given project. Case studies examining larger arrays of devices would be of interest, to investigate to what extent the LCOE can be reduced and to see how the optimum array design varies with location. Lastly the inclusion of more constraints, for example seabed sediment, marine traffic and cliff edges as cable landing obstacles, would add more realism to future case studies.

Acknowledgements

The authors wish to thank Albatern Ltd, the industrial partner of the research project, for their funding and support in sponsoring the lead author. In addition, the Energy Technology Institute (ETI) and Research Councils UK Energy Programme who have funded this research through the IDCORE programme (grant number: EP/J500847/1).

References

Allan, G., Gilmartin, M., McGregor, P., Swales, K., 2011. Levelised costs of wave and tidal energy in the UK: cost competitiveness and the importance of “banded” renewables obligation certificates. Energy Policy 39, 23–39.

Behrens, S., Hayward, J., Hemer, M., Osman, P., 2012. Assessing the wave energy converter potential for australian coastal regions. Renew. Energy 43, 210–217.

Booij, N., Ris, R.C., Holthuijsen, L.H., 1999. A third-generation wave model for coastal regions, part i, model description and validation. J. Geophys Res. 104, 7649–7666.

Boud, R., 2012. Uk Wave Resource Study. Tech. rep.. The Carbon Trust.

Cavazzi, S., Dutton, A.G., 2016. An offshore wind energy geographic information system (owe-gis) for assessment of the UK's offshore wind energy potential. Renew. Energy 87, 212–228.

Colorbrewer 2.0, 2013. Color Advice for Catography. http://colorbrewer2.org. (Accessed 25 September 2017).

Cornett, A.M., 2006. A Global Wave Energy Resource Assessment. Tech. rep.. Canadian Hydraulics Centre, National Research Council.

Dalton, G., Lewis, T., 2011. Performance and economic feasibility analysis of 5 wave energy devices off the west coast of Ireland. In: Proceedings of EWTEC11.

Dalton, G.J., Alcorn, R., Lewis, T., 2010. Case study feasibility analysis of the pelamis wave energy convertor in Ireland, Portugal and north America. Renew. Energy 35, 443–455.

Dijkstra, E.W., 1959. A note on two problems in connexion with graphs. Numer. Math. 1 (1), 269–271.

Farrell, N., Donoghue, C.O., Morrissey, K., 2015. Quantifying the uncertainty of wave energy conversion device cost for policy appraisal: an Irish case study. Energy Policy 78, 62–77.

Flocard, F., Ierodiaconou, D., Coghlan, I.R., 2016. Multi-criteria evaluation of wave energy projects on the south-east australian coast. Renew. Energy 99, 80–94.

Gray, A., 2017. Modelling Operations and Maintenance Strategies for Wave Energy Arrays (Ph.D. thesis). Industrial Doctoral Centre for Offshore Renewable Energy (IDCORE).

Gunn, K., Stock-Williams, C., 2012. Quantifying the global wave power resource. Renew. Energy 44, 296–304.

Iglesias, G., Lopez, M., Carballo, R., Castro, A., Fraguela, J., Frigaard, P., 2009. Wave energy potential in galicia (nw Spain). Renew. Energy 34, 2323–2333.

Joint Nature Conservation Committee, 2009. Marine spas. http://jncc.defra.gov.uk/page-1414. (Accessed 28 June 2017).

Kuwashima, S., Hogben, N., 1986. The estimation of wave height and wind speed persistence statistics from cumulative probability distributions. Coast. Eng. 9, 563–590.

House of Commons Energy and Climate Change Committee, 2009. Low Carbon Technologies in a Green Economy: Fourth Report of Session 2009-10. Tech. rep.

Mackay, D., 2008. Sustainable Energy - without the Hot Air. UIT Cambridge.

Mørk, G., Barstow, S., Kabuth, A., Pontes, M.T., 2010. Assessing the global wave energy potential. In: Proceedings of OMAE 2010.

Nobre, A., Pacheco, M., Jorge, R., Lopes, M., Gato, L., 2009. Geo-spatial multi-criteria analysis for wave energy conversion system deployment. Renew. Energy 34, 97–111.

Parliment and Council of European Union, 2009a. Directive 2009/28/ec of the European Parliament and of the Council on the Production of the Use of Energy from Renewable Sources. http://data.europa.eu/eli/dir/2009/28/oj.

Parliment and Council of European Union, 2009b. Directive 2009/147/ec of the European Parliament and of the Council of 30 November 2009 on the Conservation of Wild Birds. http://data.europa.eu/eli/dir/2009/147/oj.

Pontes, M.T., 1998. Assessing the european wave energy resource. J. Offshore Mech. Arct. Eng. 120, 226–231.

Prest, R., Daniell, T., Ostendorf, B., 2007. Using gis to evaluate the impact of exclusion zones on the connection cost of wave energy to the electricity grid. Energy Policy 35, 4516–4528.

Previsic, M., 2004. System Level Design, Performance and Costs for San Francisco California Pelamis Offshore Wave Power Plant. Tech. rep.. EPRI.

Reikard, G., Robertson, B., Bidlot, J.-R., 2015. Combining wave energy with wind and solar: short-term forecasting. Renew. Energy 81, 442–456.

Sierra, J., González-Marco, D., Sospedra, J., Gironella, X., Mösso, C., Sánchez-Arcilla, A., 2013. Wave energy resource assessment in lanzarote (Spain). Renew. Energy 55, 480–489.

Stallard, T., Dhedin, J.-F., Saviot, S., Noguera, C., 2010. Deliverables d7.4.1 and d7.4.2: Procedures for Estimating Site Accessibility and Appraisal of Implications of Site Accessibility. Tech. rep.. EquiMar project.

The Scottish Government, 2015. 2020 Routemap for Renewable Energy in Scotland - Update. Tech. rep.

Thorpe, T.W., 1999. A Brief Review of Wave Energy. Tech. rep.. UK Department of Trade and Industry.

Vasileiou, M., Loukogeorgaki, E., Vagiona, D.G., 2017. Gis-based multi-criteria decision analysis for site selection of hybrid offshore wind and wave energy systems in Greece. Renew. Sustain. Energy Rev. 73, 745–757.

Vazquez, A., Iglesias, G., 2016. Capital costs in tidal stream energy projects - a spatial approach. Energy 107, 215–226.

Walker, R.T., van Nieuwkoop-McCall, J., Johanning, L., Parkinson, R.J., 2013. Calculating weather windows: application to transit, installation and the implications on deployment success. Ocean. Eng. 68, 88–101.